*Aust. J. Phys.*, 1993, **46**, 601–11

# A Tight Binding Model for the Density of States of Graphite-like Structures, Calculated using Green's Functions*

*B. A. McKinnon and T. C. Choy*

Department of Physics, Monash University,
Clayton, Vic. 3168, Australia.

*Abstract*

The electronic structure of graphite-like materials is investigated within the framework of the tight binding model. The densities of states of simple hexagonal and Bernal graphite are calculated, including two layer (2D) and bulk (3D) cases. The calculation employs Green's function techniques, resulting in essentially analytic solutions in terms of elliptic integrals. The Bernal density of states is found to agree qualitatively with experimental measurements and the extension of our studies to surface effects and carbon fibre structures is also discussed.

## 1. Introduction

The aim of this work is to develop a simple model for understanding the features of the electronic density of states of graphite and graphite-like materials. In this paper we present a model which successfully describes the density of states of simple hexagonal (SH) and Bernal graphite, in a way that is both physically transparent and mathematically tractable. A further motivation for this work is that it forms a sound basis for an extension to complex phenomena such as surface effects and graphene tubules.

The model employs the parametrised tight binding (TB) Hamiltonian to describe the interaction between the electronic states, which for graphite are localised about the carbon lattice sites. The major difference between this model and other studies (McClure 1957; Slonczewski and Weiss 1958; Haering 1958; Charlier *et al.* 1991*a*) is that the density of states (DOS) is calculated using Green's functions, a technique resulting in an analytic solution in two dimensions and an essentially analytic solution in three dimensions.

Graphite has been the subject of much theoretical and experimental attention since the proposal of its structure by J. D. Bernal in 1924. The 'Bernal' graphite identified was found to consist of layers of hexagonal carbon lattices stacked in an alternate ABABAB fashion. In Fig. 1, each carbon atom is shown with four valence electrons, forming $sp^2$ hybridised $\sigma$ bonds, spaced 120° apart within the plane, with a $2p_z$ orbital perpendicular to the plane. While the $sp^2$ bonds contribute only to intra-plane bonding, the $2p_z$ orbitals contribute to $\pi$ bonding both inter- and intraplane. The inter-plane spacing is 3·35 Å, the intraplane

* Paper presented at the Festschrift Symposium for Dr Geoffrey Fletcher, Monash University, 11 December 1992.

0004-9506/93/050601$05.00

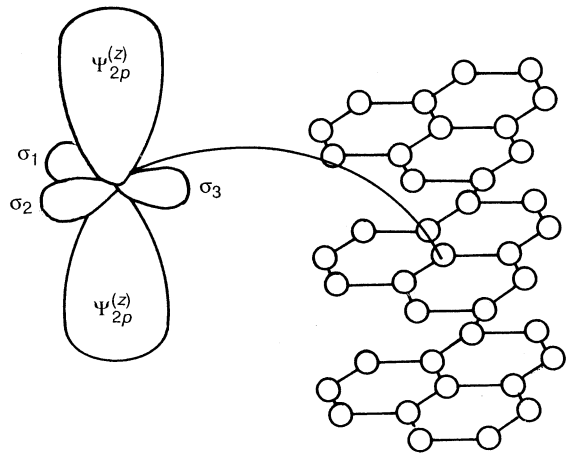


**Fig. 1.** Representation of the carbon valence orbitals: the three hybridised $\sigma$ orbitals and $\Psi_{2p}^{(z)}$, the nonhybridised $\pi$ orbital (Charlier *et al.* 1991*a*).

spacing 1·42 Å. The comparative weakness of the interplane interaction is reflected in the magnitude of the interplane spacing and the strongly anisotropic conduction properties of graphite.

Bernal graphite is but one of a wealth of graphite-like compounds. Fig. 2 illustrates three crystalline forms of graphite, of which Bernal graphite represents 80% of naturally occuring graphite, rhombohedral graphite 14%, the remaining 6% being in a turbostratic form, without any layer periodicity (Haering 1958). Although the form of graphite with the layers stacked directly above one another, SH graphite, does not occur in nature, it is useful to calculate its theoretical properties for comparison with other forms. Graphite-like compounds include intercalated graphite, where atoms such as Li are placed between the layers, dramatically affecting the electronic properties, and the exotic graphene tubules (see Fig. 3) discovered by Iijima in 1991. Graphene tubules appear to consist of cylindrical layers of graphite, with the hexagonal sheets being helically wrapped about the cylinder's axis such that the two edges meet with no overlap. Graphene tubules are potential one-dimensional conductors. The electronic properties of all these materials are of interest and hence the motivation for a simple model which can be easily extended to embrace all of the above systems.

Investigations of the theoretical properties of graphite fall into two broad categories, that of *ab initio* or first principles calculations and that of parametrised models. *Ab initio* calculations range from the Painter and Ellis (1970) pioneering LCAO band structure calculation to pseudopotential and density functional approaches (Charlier *et al.* 1991*b*). These calculations give detailed information about the electronic density of states over the full bandwidth. Following on from work by Wallace (1947), both Slonczewski and Weiss (1958) and McClure (1957) (hereafter, SWMc) developed a 3D parametrised TB model, exploiting the localised, directional nature of graphitic bonding. In this model, interaction between a site and any of its neighbours is represented by a parameter. McClure

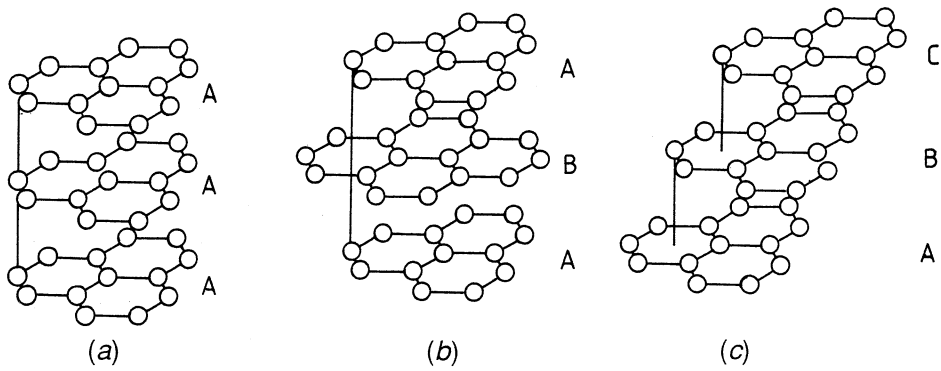


**Fig. 2.** Three crystalline structures of graphite which differ from one another by the shift imposed on the graphite planes in the stacking: (*a*) simple hexagonal graphite; (*b*) Bernal graphite; and (*c*) rhombohedral graphite (Charlier *et al.* 1991*a*).

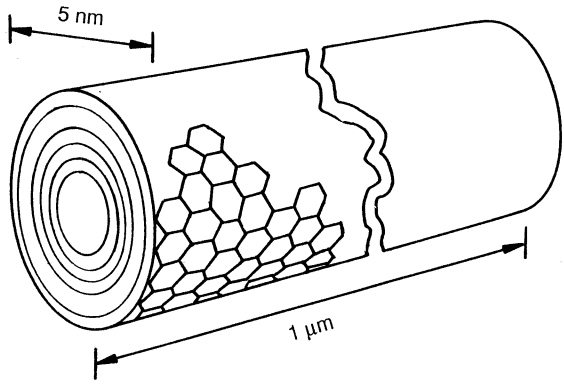


**Fig. 3.** Graphene tubule: concentric cylinder of graphite sheets wrapped helically about the cylinder's axis (see New Scientist vol. 132, p. 13, 1991).

showed that seven parameters suffice to parametrise Bernal graphite, and that the magnitudes of these parameters could be obtained from de Haas–van Alphen measurements of the Fermi surface. In graphite, the Fermi surface is very close to the edge of the Brillouin zone. SWMc used this property to determine the DOS about the Fermi level by making an expansion about the edge of the Brillouin zone, an approximation yielding accurate results at the Fermi level, but which becomes rapidly less accurate away from the Fermi level. Charlier *et al.* (1991*a*) used the SWMc method to calculate the DOS at the Fermi level for SH graphite.

In our model, we too employ a TB Hamiltonian. However, through the use of Green's functions to determine the DOS, the aforementioned approximation is avoided, and the DOS of the whole bandwidth is obtained. Thus, the Green's function technique bridges the gap between the SWMc method and the *ab initio* calculation. In addition the technique provides an essentially analytic solution. Consequently, we have been able to extend the work by Charlier *et al.* (1991*a*) on SH graphite to the whole bandwidth and to calculate the DOS for Bernal graphite. In spite of the simplicity of the model it is found that the essential features of

the experimental DOS are obtained, and that the features are easy to interpret physically, fulfilling the aims of the model.

The remainder of this paper contains, firstly, a brief explanation of the theory of the model, followed by results of calculations of the DOS for simple hexagonal and Bernal graphite. The results are compared with previous calculations and experiment. A discussion of possible extension to the study of surface effects and more complex structures such as graphene tubules is given in the final section.

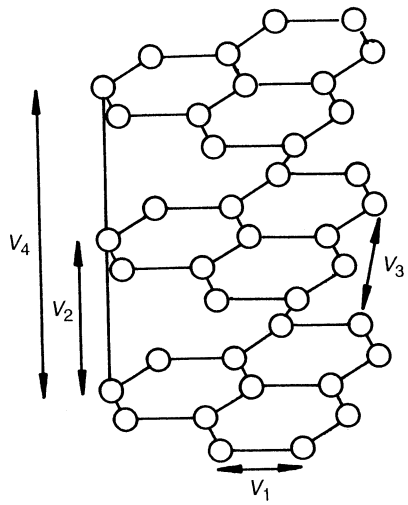


**Fig. 4.** Tight binding Hamiltonian parameters: $V_1 = 3{\cdot}2$ eV, $V_2 = 0{\cdot}4$ eV, $V_3 = 0{\cdot}04$ eV and $V_4 = 0{\cdot}04$ eV.

## 2. Theory

The model is formulated within the context of the TB Hamiltonian:

$$\hat{H} = \sum_i |\, i \,\rangle\, \epsilon_i \,\langle\, i \,| + \sum_{i,j} |\, i \,\rangle\, V_{ij} \,\langle\, j \,|\,, \tag{1}$$

which is in a Wannier representation; that is, $\langle\, r \,|\, i \,\rangle$ is a wavefunction localised about site $i$. Given the nature of carbon bonding in a graphite lattice, this is an appropriate Hamiltonian, with the intersite interactions $V_{ij}$ (see Fig. 4) being nonzero only for nearest and next nearest neighbours. We use the same magnitudes for the parameters $V_{ij}$ as Charlier *et al.* (1991*a*). The calculation is also performed with reference to the constant site energy $\epsilon_i$, hereafter taken as $\epsilon_i = 0$.

SWMc showed that the bands due to the $\pi$ and $\sigma$ bands only have a small degree of overlap so that it is reasonable to consider the $\pi$ DOS separately from that of the $\sigma$ DOS. This is reflected in the band calculation by Painter and Ellis (1970), where the $\pi$ bands were found to be situated either side of the Fermi level and thus responsible for the conduction properties. Hence we shall limit our calculation to that of the DOS of the $\pi$ band.

The eigenfunctions and eigenvalues of the Hamiltonian are

$$|\, k \,\rangle = \sum_j \mathrm{e}^{\mathrm{i}\boldsymbol{k}\cdot\boldsymbol{r}_j} \,|\, j \,\rangle\,, \qquad E(\boldsymbol{k}) = \sum_{\boldsymbol{R}_l} V_{0l} \mathrm{e}^{\mathrm{i}\boldsymbol{k}\cdot\boldsymbol{R}_l}\,, \tag{2}$$

respectively. The sum on $j$ is over all lattice sites, and the sum on $\boldsymbol{R}_l$ over the lattice basis vectors.

It is well known that the DOS,

$$N(E) = \sum_{\boldsymbol{k}} \delta\big(E - E(\boldsymbol{k})\big)\,, \tag{3}$$

is proportional to the imaginary part of the single-particle, time-independent Green's function connecting a state to itself, i.e.

$$N(E) = -\frac{1}{\pi}\,\mathrm{Im}\Big\{\mathrm{Tr}\Big[\lim_{\epsilon\to 0^+} G(\boldsymbol{r},\boldsymbol{r};E+\mathrm{i}\epsilon)\Big]\Big\}\,. \tag{4}$$

The definition of the Green's function operator is

$$\hat{G}(t) = \frac{1}{t\hat{I}-\hat{H}} = \sum_{\boldsymbol{k}} \frac{|\,\boldsymbol{k}\rangle\langle\,\boldsymbol{k}\,|}{t-E(\boldsymbol{k})}\,, \tag{5}$$

where $t = E + \mathrm{i}\epsilon$. The Green's function connecting a lattice site $\boldsymbol{l}$ to itself is then

$$G(\boldsymbol{l},\boldsymbol{l};t) = \sum_{\boldsymbol{k}} \frac{\langle\boldsymbol{l}\,|\,\boldsymbol{k}\rangle\,\langle\,\boldsymbol{k}\,|\,\boldsymbol{l}\rangle}{t-E(\boldsymbol{k})}\,, \tag{6}$$

which can be converted to a continuous sum over the first Brillouin zone. The DOS is then just the imaginary part of the trace of this function in the limit as $\epsilon \to 0^+$. For the graphite monolayer or honeycomb lattice, Horiguchi (1972) showed that the Green's function and hence the DOS are expressible analytically in terms of complete elliptic integrals of the first kind.

## 3. Results

*(a) The Graphite Monolayer*

Before considering the 3D graphite structure it is instructive to look at the DOS of a single layer. The hexagonal or honeycomb lattice is composed of two site types, which form two interpenetrating triangular lattices. The Hamiltonian eigenfunctions can thus be split into two groups, one summing over sites of type A and the other over sites of type B. The two sites result in two energy bands. Allowing only nearest neighbour interactions $V_1$, the matrix representation of the operator $t\hat{I}-\hat{H}$, in terms of these eigenfunctions, is

$$\begin{bmatrix} t & -\mu V_1 \\ -\mu^* V_1 & t \end{bmatrix}\,, \tag{7}$$

where $\mu = \exp(ik_x a) + \exp[i(-k_x a/2 + k_y\sqrt{3}a/2)] + \exp[i(-k_x a/2 - k_y\sqrt{3}a/2)]$ and simply reflects the geometry of the problem, $a$ being the length of a hexagon side, and $\mu^*$ is its complex conjugate. The DOS is then calculated by taking the trace of the inverse of the matrix $(t\hat{I} - \hat{H})$. Hence the total DOS becomes

$$\rho(E) = -\frac{1}{\pi}\,\mathrm{Im}\left[\lim_{\epsilon\to 0^+}\int_{1st\mathrm{BZ}} \mathrm{d}\boldsymbol{k}\,\frac{t}{t^2 - |\,\mu\,|^2\,V_1^2}\right], \tag{8}$$

which has the form of an elliptic integral (Horiguchi 1972).

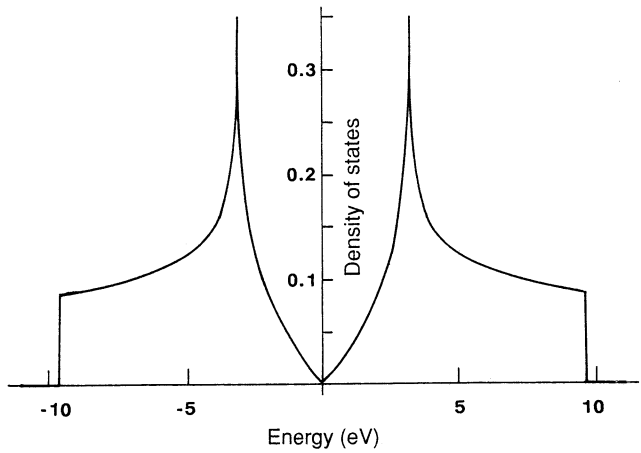


**Fig. 5.** Density of states for the graphite monolayer: $V_1 = 3{\cdot}2$ eV.

Fig. 5 shows the 2D DOS for the honeycomb lattice. The bandwidth of the DOS is $6V_1$, hence $V_1$ controls the bandwidth and is a measure of the degree to which hopping between nearest neighbours is facilitated. In graphite, the Fermi level is very close (within $0{\cdot}024$ eV—see Charlier *et al.* 1991*b*) to $\epsilon_i$, so that $E = 0$ approximates the Fermi level. Because the effective width of the bandgap at $\epsilon_F$ is zero, the graphite monolayer is classified as a zero-overlap semi-metal, in that it is neither conductor nor insulator. The honeycomb DOS exhibits the expected logarithmic 2D Van Hove singularities and is symmetrical about $E = 0$, a consequence of the bipartite nature of the lattice.

*(b) Two-layer Results*

Having now understood the essential features of the DOS for a single layer, it is interesting to see how the addition of another layer affects the DOS. This is still effectively a two-dimensional calculation, however, now the interaction $V_2$ between atoms directly above one another is included. The total DOS becomes

$$\rho(E) = -\frac{1}{\pi}\,\mathrm{Im}\left[\lim_{\epsilon\to 0^+}\int_{1st\mathrm{BZ}} \mathrm{d}\boldsymbol{k}\left\{\frac{t + V_2}{(V_2 + t)^2 - |\,\mu\,|^2\,V_1^2} + \frac{t - V_2}{(t - V_2)^2 - |\,\mu\,|^2\,V_1^2}\right\}\right], \tag{9}$$

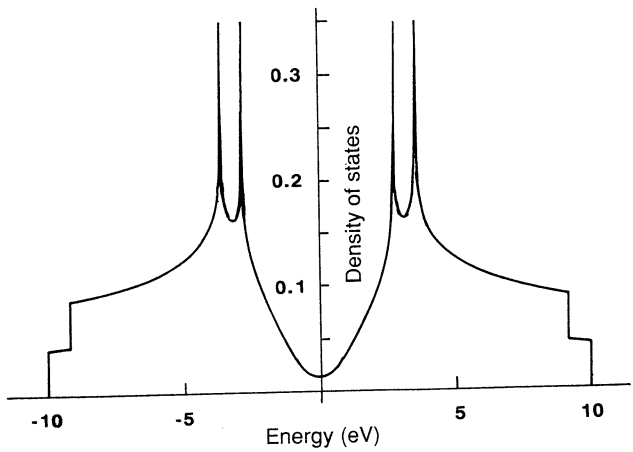


**Fig. 6.** Density of states for two graphite layers: $V_1 = 3{\cdot}2$ eV and $V_2 = 0{\cdot}4$ eV.

which, as can been seen from Fig. 6, consists of the sum of two single-layer DOS, one shifted by $+V_2$, the other by $-V_2$. The most dramatic consequence is that the DOS at the Fermi level becomes nonzero, and thus metallic. In addition, corresponding to the increase in allowed interaction, the bandwidth increases by $2V_2$. The larger $V_2$, the larger the degree of interaction, so the larger the bandwidth and the magnitude of the DOS at the Fermi level. From these results we would expect that when an infinite number of layers are stacked directly above the first, forming SH graphite, it would correspond to the sum over an infinite number of monolayer DOS shifted from $-V_2$ to $+V_2$. In fact, in the bulk material, because each layer interacts with both the layers above and below it, the DOS consists of the sum of an infinite number of monolayer DOS shifted between $-2V_2$ and $+2V_2$.

*(c) Simple Hexagonal Graphite*

The DOS for SH graphite with the inclusion of various levels of interaction is shown in Fig. 7. It corresponds to the following integral:

$$\rho(E) = -\frac{1}{\pi}\,\mathrm{Im}\left[\lim_{\epsilon\to 0^+}\int_{1st\mathrm{BZ}} \mathrm{d}\boldsymbol{k} \times \frac{t + 2V_2\cos(k_z c) + 2V_4\cos(2k_z c)}{[t + 2V_2\cos(k_z c) + 2V_4\cos(2k_z c)]^2 - |\,\mu\,|^2\,[V_1 + 2V_3\cos(k_z c)]}\right], \tag{10}$$

where $c$ is the interlayer spacing. The DOS exhibits the expected 3D Van Hove features and a finite bandwidth. The effect of $V_3$ is to make the DOS asymmetric about $\epsilon_F$, which is a consequence of the lattice no longer being bipartite. Parameter $V_4$ effectively increases the strength of the interplane interaction, hence exaggerating the effect of $V_2$. In Fig. 8 the DOS obtained by Charlier *et al.* (1991*a*) is overlaid with our Green's function technique results, where it can be observed that there is excellent agreement about the $\epsilon_F$ point, but divergence away from $\epsilon_F$. Thus our results retain the accuracy about the Fermi level of the SWMc method, as well as giving information about the whole bandwidth.

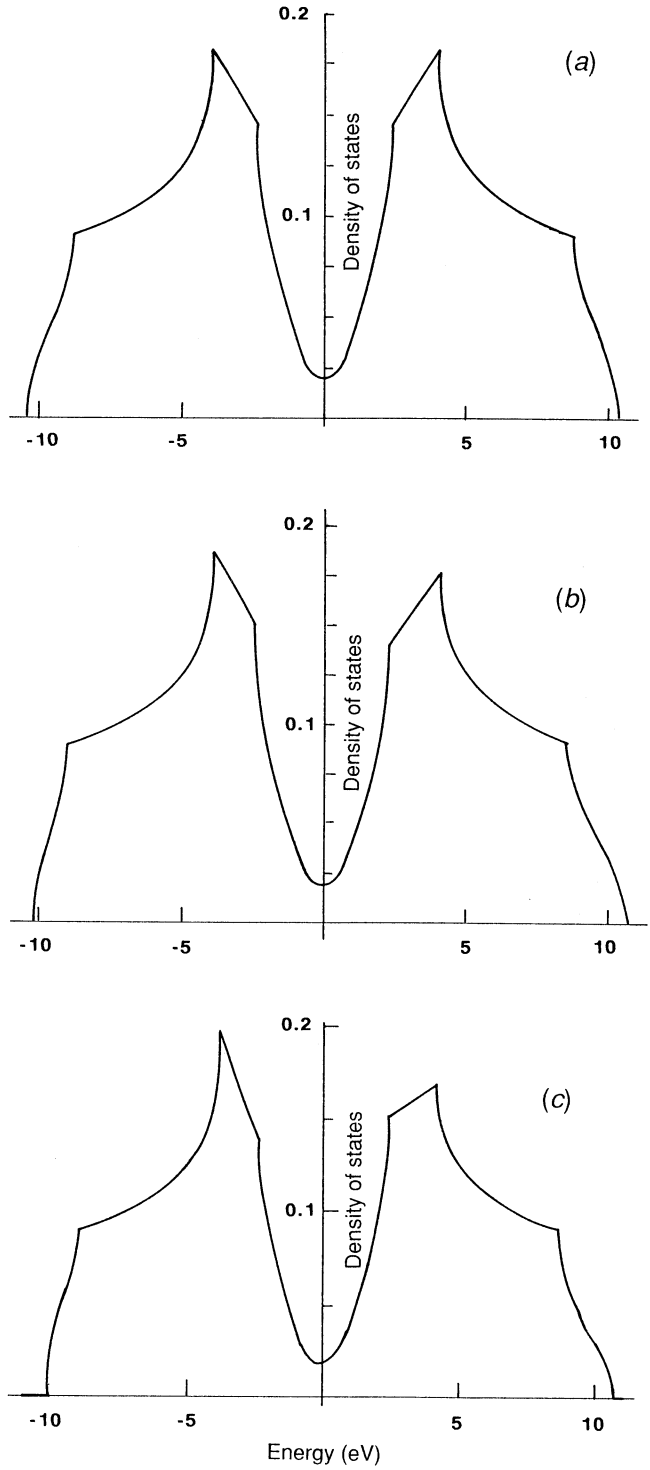


**Fig. 7.** Density of states for simple hexagonal graphite: (*a*) including $V_1$ and $V_2$; (*b*) including $V_1$, $V_2$ and $V_3$; and (*c*) including $V_1$, $V_2$, $V_3$ and $V_4$.

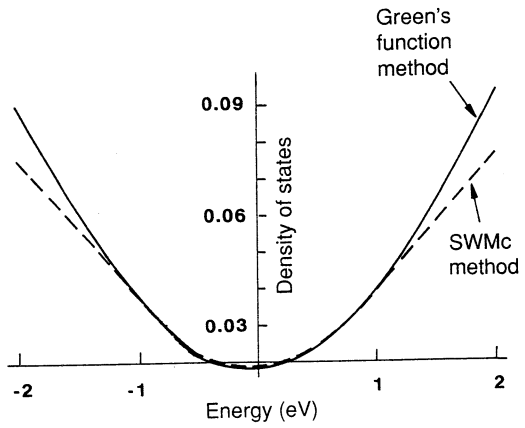


**Fig. 8.** Comparison of results with those obtained by the SWMc method.

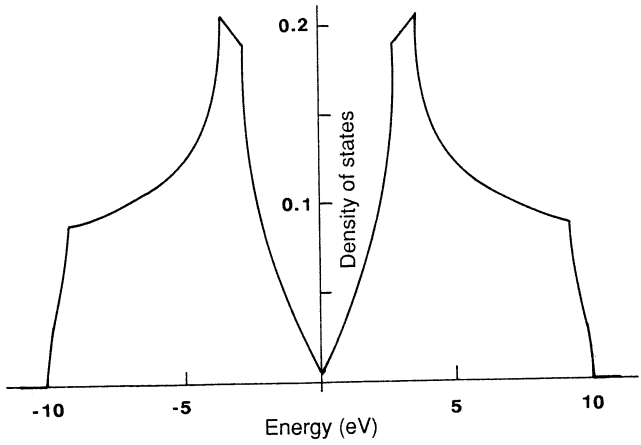


**Fig. 9.** Calculated density of states for Bernal graphite: $V_1 = 3{\cdot}2$ eV and $V_2 = 0{\cdot}4$ eV.

*(d) Bernal Graphite*

In Fig. 9 we show the DOS for Bernal graphite, obtained using Green's function techniques. As can be seen from the corresponding integral,

$$\rho(E) = -\frac{1}{\pi}\,\mathrm{Im}\left[\lim_{\epsilon\to 0+}\int_{1st\mathrm{BZ}} \mathrm{d}\boldsymbol{k}\left\{\frac{t - V_2\cos(k_z c)}{t[t - 2V_2\cos(k_z c)] - |\,\mu\,|^2\,V_1^2} + \frac{t + V_2\cos(k_z c)}{t[t + 2V_2\cos(k_z c)] - |\,\mu\,|^2\,V_1^2}\right\}\right], \quad (11)$$

we have only included $V_1$ and $V_2$ interactions because the inclusion of more interactions resulted in the loss of an analytic solution. The main features of the

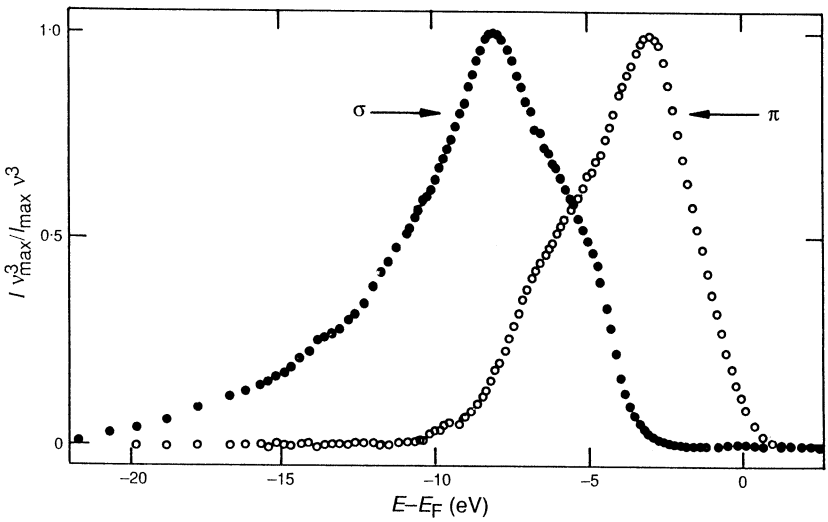


**Fig. 10.** X-ray emission spectrum for monocrystalline graphite. The $\pi$ and $\sigma$ band spectra are normalised to the same height (Kieser 1977).

results are a peak between 2·8 and 3·6 eV, a bandwidth of 20 eV and a finite DOS at $\epsilon_F$. Despite the inclusion of only two parameters, the calculated DOS compares favourably with the experimental X-ray emission spectrum obtained by Kieser in 1977 (see Fig. 10). This is a reflection of the highly localised and anisotropic nature of the interatomic bonding. Kieser exploited the polarisation of the emitted X-ray to separate the $\pi$ and $\sigma$ band DOS. An X-ray emission spectrum is obtained by using a primary X-ray beam to excite a valence electron to the conduction band, and detecting the subsequent X-ray due to de-excitation. The cross section for this process can be related via Fermi's Golden rule to the square of the matrix element for the transition, multiplied by the electronic density of states. Because the bonds are so strongly directional, the radiation emitted is found to be polarised depending on whether it is due to de-excitation from a $\pi$ or $\sigma$ state. Thus Kieser was able to decompose the X-ray spectrum into $\pi$ and $\sigma$ band DOS. The $\pi$ band exhibits a peak between 2·5 and 3·5 eV, a shoulder at 7 eV, and a half-bandwidth of 9·5 eV. While the features of the calculated and experimental DOS compare qualitatively, the calculated spectrum would agree with experiment more closely if the peaks were marginally closer to $\epsilon_F$ and the bandwidth were slightly smaller. Both of these features are largely determined by the intraplane interaction, i.e. $V_1$, hence a smaller $V_1$ would improve the agreement.

## 4. Conclusion

We have shown that the Green's function model is able to give a reasonably correct description of the DOS, with the input of only two parameters, the interaction of nearest neighbours inter- and intra-plane. This work has extended earlier TB model studies of graphite to encompass the whole $\pi$ bandwidth. The true power of the method, however, lies in the uses of Green's function techniques. These techniques can be used to extend the model to surface states, as was

established by Foo *et al.* (1976). Surface states arise when the system is no longer entirely a bulk system, but, for example, one with a defined edge. The problem can be treated in a manner analagous to that of Section 3*b*, where each layer is considered separately. Foo *et al.* have shown that the resultant finite layer DOS converges to the bulk result. This is an important extension of the Green's function technique, as many experimental methods, such as secondary electron emission spectroscopy (Willis *et al.* 1974), probe only a small number of layers and are influenced by surface properties. We are also investigating the extension of the model to the DOS of graphene tubules. While there has been much work done on graphene tubule band structure (Hamada *et al.* 1992; Saito *et al.* 1992), the effect of curvature, helical winding and multiple layers on the DOS remains to be studied.

**Acknowledgment**

B.A.McK. acknowledges the support of an APRA scholarship.

**References**

Bernal, J. D. (1924). *Proc. R. Soc. London* A **106**, 749.
Charlier, J.-C., Gonze, X., and Michenaud, J.-P. (1991*a*). *Phys. Rev.* B **43**, 4579.
Charlier, J.-C., Michenaud, J.-P., Gonze, X., and Vigneron, J.-P. (1991*b*). *Phys. Rev.* B **44**, 13237.
Foo, E-Ni, Thorpe, M. F., and Weaire, D. (1976). *Surf. Sci.* **57**, 323.
Haering, R. R. (1958). *Can. J. Phys.* **36**, 352.
Hamada, N., Sawada, S., and Oshiyama, A. (1992). *Phys. Rev. Lett.* **10**, 1579.
Horiguchi, T. (1972). *J. Math. Phys.* **13**, 1411.
Iijima, S. (1991). *Nature* **354**, 56.
Kieser, J. (1977). *Z. Phys.* B **26**, 1.
McClure, J. W. (1957). *Phys. Rev.* **108**, 612.
Painter, G. S., and Ellis, D. E. (1970). *Phys. Rev.* B **1**, 4747.
Saito, R., Fujita, M., Dresselhaus, G., and Dresselhaus, M. S. (1992). *Phys. Rev.* B **46**, 1804.
Slonczewski, J. C., and Weiss, P. R. (1958). *Phys. Rev.* **109**, 272.
Wallace, P. R. (1947). *Phys. Rev.* **71**, 622.
Willis, R. F., Fitton, B., and Painter, G. S. (1974). *Phys. Rev.* B **9**, 1926.

Manuscript received 8 February, accepted 7 April 1993